Synthesis, electrochemical investigation and EPR spectroscopy of a reversible four-stage redox system based on mesoionic 5,5′-azinobis(1,3-diphenyltetrazole) and related mesoionic compounds †

Shuki Araki,*[a] Kaori Yamamoto,[a] Tomoko Inoue,[a] Koji Fujimoto,[a] Hatsuo Yamamura,[a] Masao Kawai,[a] Yasuo Butsugan,[a] Jinkui Zhou,[b] Emerich Eichhorn,[b] Anton Rieker*[b] and Martina Huber[c]‡

[a] *Department of Applied Chemistry, Nagoya Institute of Technology, Gokiso-cho, Showa-ku, Nagoya 466-8555, Japan*
[b] *Institute of Organic Chemistry, University of Tübingen, Auf der Morgenstelle 18, D-72076 Tübingen, Germany*
[c] *Institute of Organic Chemistry, Free University of Berlin, Takustr. 3, D-14195 Berlin, Germany*

Received (in Cambridge) 1st December 1998, Accepted 17th February 1999

Mesoionic 5,5′-azinobis(1,3-diphenyltetrazole) **1** was prepared, and its chemical oxidation gave stable crystals of the corresponding radical cation $\mathbf{1}^{\bullet+}$ and dication $\mathbf{1}^{2+}$, which reversibly gave back azine **1** on reduction with zinc. Electrochemical investigations of **1** using cyclovoltammetry and differential pulse voltammetry in pyridine (Py) or dichloromethane (DCM) also revealed the two reversible successive one-electron oxidations leading to dication $\mathbf{1}^{2+}$ *via* radical cation $\mathbf{1}^{\bullet+}$, both of which can be reduced to the neutral state **1**. In the cathodic process, **1** was reduced by two consecutive one-electron transfers at only slightly different potentials up to the corresponding dianion $\mathbf{1}^{2-}$ which could be re-oxidized to the neutral state; thus constituting a reversible four-stage redox system. Radical cation $\mathbf{1}^{\bullet+}$ and anion $\mathbf{1}^{\bullet-}$ were characterized by EPR spectroscopy. In order to get more insights into the spin-density distribution of $\mathbf{1}^{\bullet+}$, the bis- and tetra-^{15}N-labelled species $\mathbf{1a}^{\bullet+}$, $\mathbf{1b}^{\bullet+}$ and $\mathbf{1c}^{\bullet+}$ were synthesized and investigated by EPR and ^{15}N as well as ^{14}N ENDOR spectroscopy, revealing that the largest N hyperfine coupling constants are due to the nitrogen atoms of the central bridge. According to ^{1}H ENDOR there seems to be a small coupling with the protons of both phenyl rings which cannot be resolved in the EPR spectrum.

The electrochemical properties of the related mesoionic compounds **5**–**10** were also investigated in Py or DCM solutions. In the cathodic process, a reduction peak of **9** and **10** was observed due to their reversible one-electron reduction to the corresponding radical anions. The radical obtained on reduction of **10** was characterized by EPR spectroscopy. On the other hand, **5**–**8** can be reduced by a formal two-electron transfer up to the corresponding dianions which are re-oxidizable to the neutral state. In the anodic process, **9/10** undergo irreversible one-electron oxidations whereas **5/6** (in DCM) and **7/8** (in Py) experience reversible or irreversible step by step two-electron oxidations leading to the dications. In Py the oxidation products of **5/6** react to further species revealing two more oxidation and several rereduction peaks. On the other hand, the oxidation products of **7/8** are instable in DCM (one main oxidation and rereduction peak). The electrochemical data are discussed in terms of delocalization in the cations and conjugation in the dications.

Introduction

Mesoionic compounds are an interesting family of heterocyclic compounds. Their unique properties, such as reaction behaviour, structural characteristics, and biological activities, have attracted much attention, and a wide variety of derivatives have so far been studied.[1] However, their electrochemical properties have gathered relatively little attention. In this paper is described the synthesis of mesoionic 5,5′-azinobis(1,3-diphenyltetrazole) **1** which was found to undergo reversible transfer of electrons constituting a novel four-stage redox system. Radical cation $\mathbf{1}^{\bullet+}$ and dication $\mathbf{1}^{2+}$ were isolated in crystalline form, and the radical cation and radical anion of **1** were characterized by EPR spectroscopy. The phenylogue-type analogues **5**–**8** of mesoionic azine **1** were also prepared and their chemical and electrochemical redox reactions were investigated, in comparison with mesoionic azine **1,** by means of cyclovoltammetry (CV) and differential pulse voltammetry (DPV).

Results and discussion

Synthesis and chemical reactions

We have recently found that a 5-chloro-1,3-diphenyltetrazolium salt readily undergoes substitution reactions with nitrogen-nucleophiles.[2,3] By mixing with hydrazine hydrate, the chlorotetrazolium ion readily gave purple mesoionic azine **1** in good yield [eqn. (1)]. ^{1}H and ^{13}C NMR chemical shifts of the 1,3-diphenyltetrazolium ring protons and carbons of **1** are similar

† Supplementary data are available (SUPPL. NO. 57507, pp. 6) from the British Library. For details of the Supplementary Publications Scheme, see 'Instructions for Authors', *J. Chem. Soc.*, *Perkin Trans. 2*, available *via* the RSC web pages (http://www.rsc.org/authors). For direct electronic access see http://www.rsc.org/suppdata/p2/1999/985.

‡ *Present address*: Laboratory of Astronomy and Physics, MAT Group, Leiden University, PO Box 9504, 2300 RA Leiden, The Netherlands.

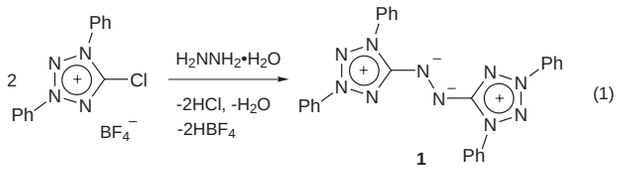

(1)

to those of the previously prepared mesoionic tetrazolium systems,[2,3] thus supporting the tetrapolar structure of azine **1**. Methylation of **1** with methyl iodide gave the *N*-methylated mesoionic cation **2** [eqn. (2)]. Even with an excess of methyl

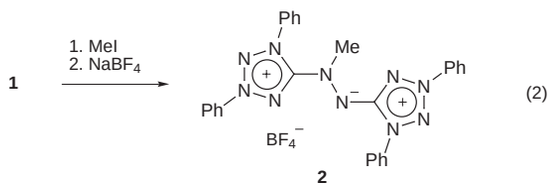

(2)

iodide, the dimethylated compound was not formed. On the other hand, azine **1** was protonated step by step; thus, with a limited amount of acetic acid brownish orange crystals of monocation **3** were formed, and with trifluoroacetic acid the colourless dication **4** was obtained. Compounds **3** and **4** regenerated the conjugate base **1** reversibly on treatment with a base like NaOH (Scheme 1). Oxidation of **1** with lead tetra-

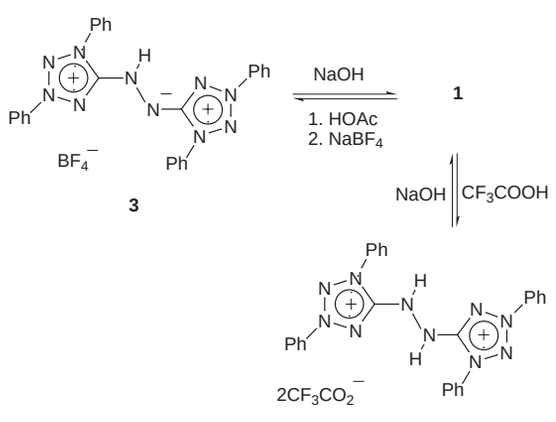

Scheme 1

acetate gave the radical cation $\mathbf{1}^{\bullet+}$ as greenish-brown crystals. Radical cation $\mathbf{1}^{\bullet+}$ is extremely stable; it could be purified by column chromatography on silica gel and stored under air for several months without appreciable decomposition. Further oxidation of $\mathbf{1}^{\bullet+}$ with conc. nitric acid gave the orange dication $\mathbf{1}^{2+}$. The longest-wavelength absorption of **1** in MeCN lies at 542 nm which shifts bathochromically to 625 nm (shoulder) on oxidation to $\mathbf{1}^{\bullet+}$, whereas further oxidation to $\mathbf{1}^{2+}$ results in a hypsochromic shift to 446 nm. Reduction of $\mathbf{1}^{\bullet+}$ and $\mathbf{1}^{2+}$ with zinc powder gave back **1**; thus, the azine constitutes a reversible redox system, and the three oxidation states (**1**, $\mathbf{1}^{\bullet+}$ and $\mathbf{1}^{2+}$) were isolated in crystalline form (Scheme 2). It should be noted

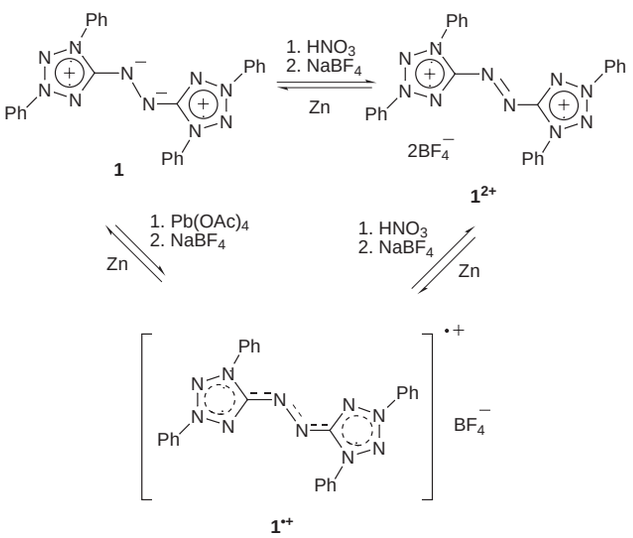

Scheme 2

that $\mathbf{1}^{2+}$ was gradually converted to $\mathbf{1}^{\bullet+}$ merely by dissolving in organic solvents such as acetonitrile and ethanol, indicating the large stability of radical cation $\mathbf{1}^{\bullet+}$. Although **1** undergoes a reversible electrochemical reduction (see below), the chemical reduction of **1** with zinc powder gave a complex mixture, from which no defined products could be isolated.

The benzene-ring inserted analogues **5**–**8** were similarly synthesized from the 5-chloro-1,3-diphenyltetrazolium ion and appropriate aromatic amines [eqn. (3)]. (1,3-Diphenyltetrazolium-5-yl)-anilide[2] (**9**) and -amide[3] (**10**) were used as reference

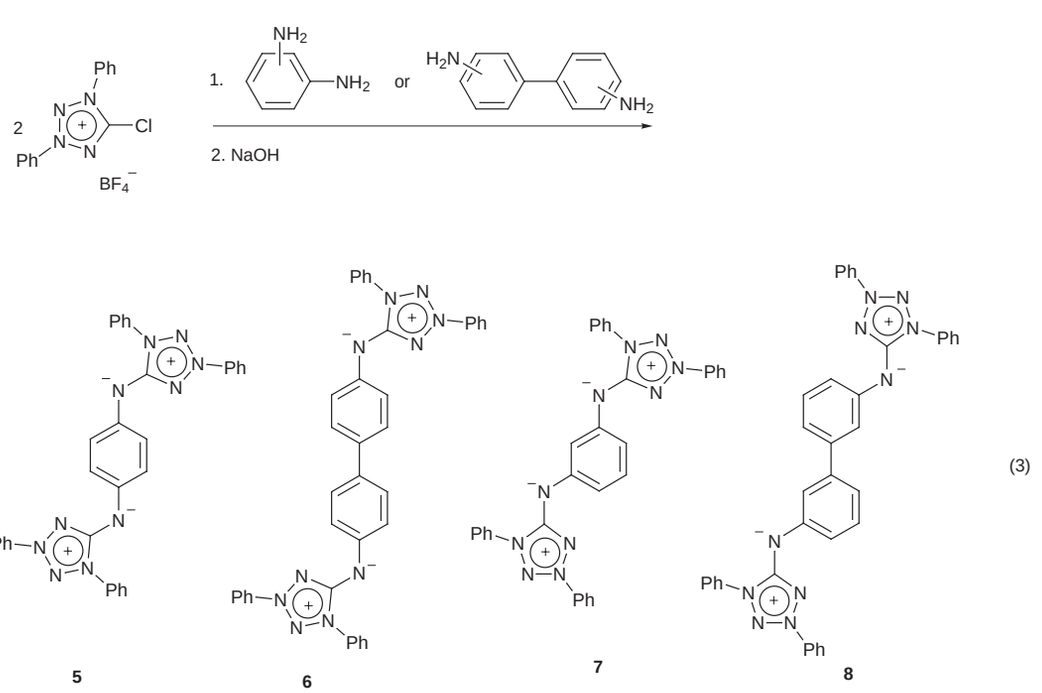

(3)

Table 1 Formal and peak potentials of the electrochemical processes of the mesoionic compounds **1** and **5**–**10**[a]

Compound	Solvent	E_{1r}/mV	E_{2r}/mV	E_{1o}/mV	E_{2o}/mV	E_{3o}/mV	E_{4o}/mV
1	Py	−1853[b]	−1967[b]	−243[b]	519[b]		
1	DCM	−1856[b]	−2006[b]	−136[b]	610[b]		
5	Py	−1805[b]		3[b]	227[b]	598[b]	870[b]
5	DCM	−1809[b]		61[b]	340[b]		
6	Py	−1755[b]		266[c]	414[c]	624[c]	858[c]
6	DCM	−1738[b]		333[b]	414[b]		
7	Py	−1792[b]		350[d]	620[b]		
7	DCM	−1809[b]		323[c]			
8	Py	−1750[b]		588[d]	771[d]		
		−1730[c]		544[c]	705[c]		
8	DCM	−1756[b]		646[d]			
		−1736[c]		573[c]			
9	Py	−1775[b]		565[c]			
10	Py	−1876[b]		1020[d]			
				1027[c]			
10	DCM	−1885[b]		1042[d]			
				974[c]			

[a] Potentials are given *vs.* $Ag/AgClO_4$ (0.01 M in MeCN–0.1 M Bu_4NPF_6). [b] E_r and E_o were obtained by averaging of the corresponding anodic and cathodic peak potentials. The potential separations ΔE between reduction and re-oxidation (or oxidation and re-reduction) peaks lie between 65 and 110 mV (in Py at $v = 0.05$ V s^{-1}). [c] E_r and E_o were obtained by DPV. [d] E_o are peak potentials of irreversible ET processes.

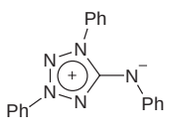

9

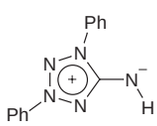

10

compounds. In contrast to the easy oxidation of **1**, the phenylogue **5** resists chemical oxidation with various oxidants, such as conc. nitric acid, lead dioxide, and alkaline potassium ferricyanate. On the other hand, reduction of **5** with zinc went smoothly and deep-red crystals of **11** were obtained. Spectroscopic data show that, contrary to the reversible electrochemical reduction (see below), one of the tetrazolium rings of **5** was reductively cleaved to *N*-substituted *N′*-phenylguanidine [eqn. (4)]. Similarly, zinc reduction of **9** gave *N*,*N′*-diphenylguanidine in good yield.

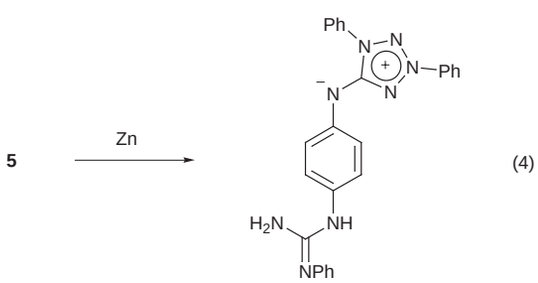

(4)

11

Electrochemical investigations

The voltammetric investigations of **1** and **5**–**10** were performed in pyridine (Py) or dichloromethane (DCM) solutions containing 0.1 M Bu_4NPF_6, at room temperature under an argon atmosphere. Py was chosen as solvent to prevent protonation and disproportionation reactions in the cathodic voltammetric process. The anodic voltammograms, however, generally are more reversible in DCM, presumably, because DCM unlike Py does not act as a strong nucleophile towards cations and dications. The cyclovoltammograms (at scan rates of 50 or 100 mV s^{-1}) and differential pulse voltammograms of **1**, **5**, **7** and **10** for cathodic and anodic processes are shown in Fig. 1–4. The potential data of **1** and **5**–**10** are summarized in Table 1. The number of electrons involved in the electrochemical processes was confirmed by controlled-potential electrolysis (CPE).

Let us first discuss the *reductions*. The cyclovoltammogram

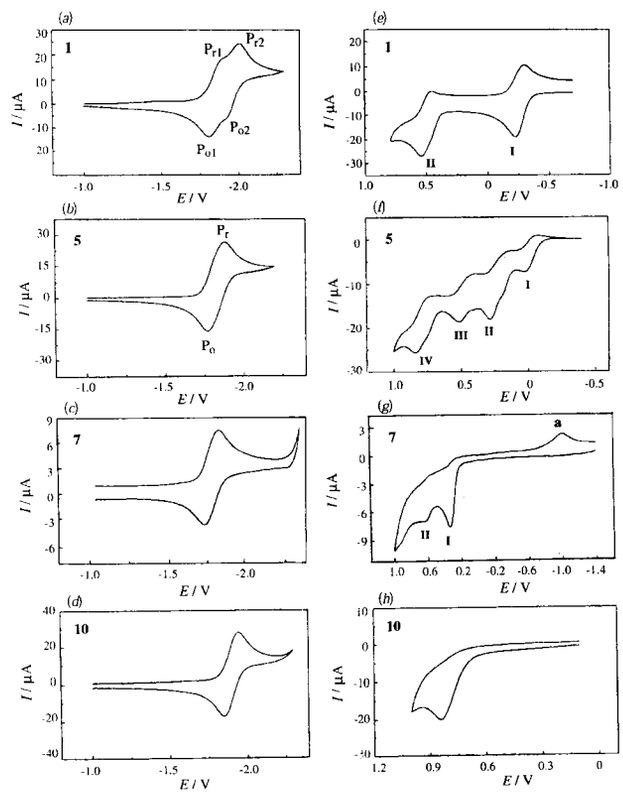

Fig. 1 CVs of cathodic reduction (*a*)–(*d*) and anodic oxidation (*e*)–(*h*) of **1**, **5**, **7** and **10** in Py solution containing 0.1 M Bu_4NPF_6; potential *vs.* $Ag/AgClO_4$ (0.01 M in acetonitrile–0.1 M Bu_4NPF_6); (*a*) **1**, (*b*) **5**, (*c*) **7**, (*d*) **10**, (*e*) **1**, (*f*) **5**, (*g*) **7** and (*h*) **10**; scan rate, 100 mV s^{-1} for (*a*), (*b*), (*d*), (*e*), (*f*) and (*h*), and 50 mV s^{-1} for (*c*) and (*g*).

of **1** [Fig. 1(*a*)] reveals two (quasireversible) couples P_{r1}/P_{o1} and P_{r2}/P_{o2} with only small potential separation between P_{r1} and P_{r2}. The corresponding DPV curves [Fig. 2(*a*)] exhibit well-separated peaks P_{r1} and P_{r2} on the first scan and P_{o1} and P_{o2} on the second scan (not shown). Obviously, there are two successive one-electron transfers to form the dianion *via* the monoanion (for EPR measurements see below). Presumably, the electrons are entering both tetrazolium rings, step by step. These rings are largely independent of each other, therefore, their reduction potentials are close together. The anions can be reoxidized to the neutral state (Scheme 3).

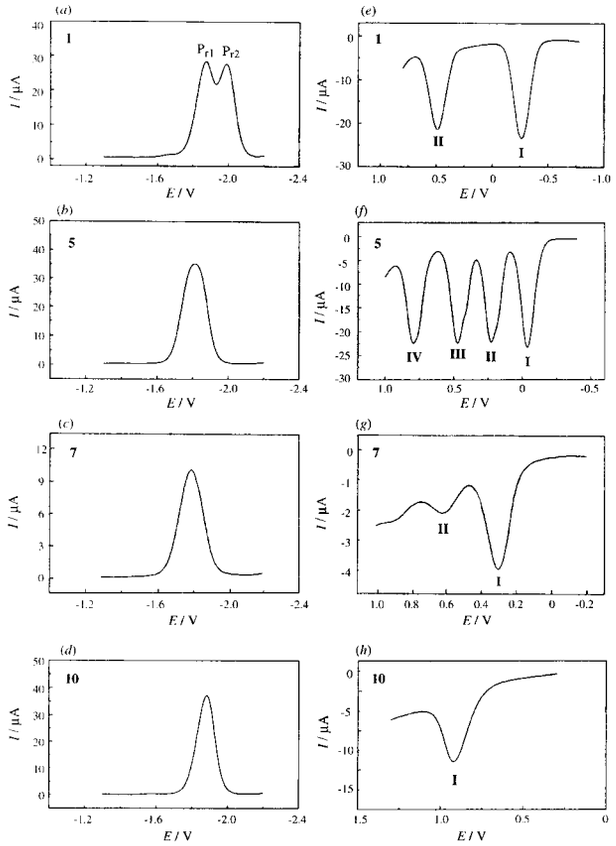

Fig. 2 DPVs of cathodic reduction (*a*)–(*d*) and anodic oxidation (*e*)–(*h*) of **1**, **5**, **7** and **10** in Py solution containing 0.1 M Bu_4NPF_6; potential *vs.* $Ag/AgClO_4$ (0.01 M in acetonitrile–0.1 M Bu_4NPF_6); scan rate, 20 mV s^{-1}; pulse amplitude, 50 mV; pulse width, 50 ms; pulse period, 200 ms; (*a*) **1**, (*b*) **5**, (*c*) **7**, (*d*) **10**, (*e*) **1**, (*f*) **5**, (*g*) **7** and (*h*) **10**.

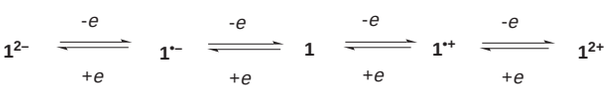

Scheme 3

In contrast to **1**, compounds **5**–**10** exhibit only one couple of reduction and reoxidation peaks (P_r and P_o) each in their voltammograms [Fig. 1(*b*) for **5**, 1(*c*) for **7**, 1(*d*) for **10**], but the DPV curves of **5**–**8** [Fig. 2(*b*) for **5**, 2(*c*) for **7**] show much broader peaks than those of **9** and **10** [Fig. 2(*d*) for **10**]. Obviously, there are two nearly simultaneous one-electron reductions of **5**–**8** being a consequence of the larger separation of the tetrazolium rings in **5**–**8** as compared to **1**, whereas the peak couples of **9** and **10** correspond to one-electron transfers each. Thus, in the first step in all cases a one-electron transfer occurs to form the radical anions. A second one-electron transfer to give the dianions follows in the case of **1** and **5**–**8**, however, only in the case of **1** the second electron-transfer occurs at noticeably larger potential.

As we can see from Table 1, the (first) reduction potential does not much vary with the type of compounds or with the solvent (Py, DCM). This indicates that the tetrazolium system acts as the pitfall for the electrons. However, Py seems to relieve the electron-transfer to a small extent. Also, insertion of aromatic systems at the *exo*-nitrogen lowers the potential, *e.g.* **1**→**5**, **1**→**7**, **10**→**9**. Interestingly, a biphenylene bridge is more effective than a phenylene bridge (**5**→**6**, **7**→**8**), and there is practically no difference between a *p*- and a *m*-arylene bridge. This may be a consequence of the larger distance between the centres of negative charge in the latter cases (**6** and **8**) resulting in a lower energy of the corresponding dianions.

In the *oxidation process*, the species show stronger diversities. Compound **1** exhibits two successive reversible one-electron

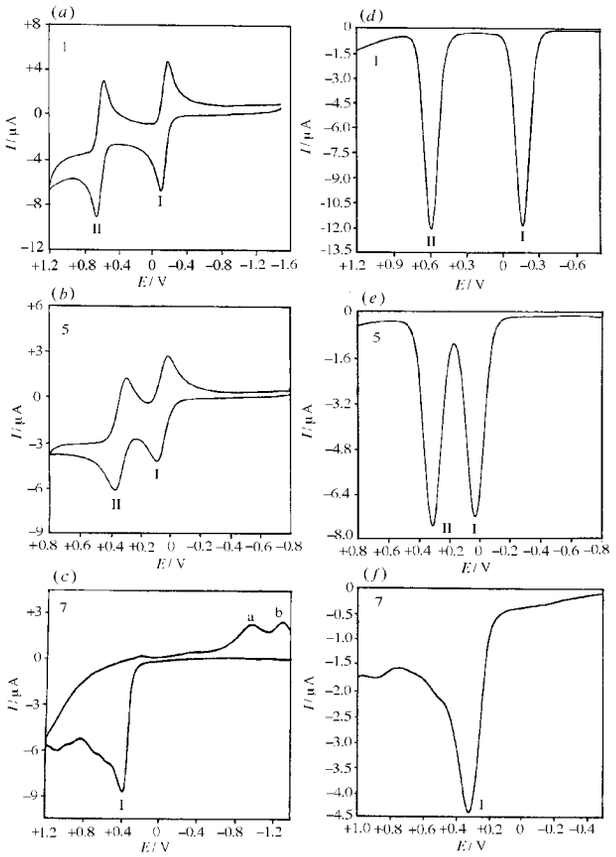

Fig. 3 CVs of the anodic oxidation (*a*)–(*c*) and their corresponding DPVs (*d*)–(*f*) of the compounds **1**, **5** and **7** in DCM solution, containing 0.1 M Bu_4NPF_6, potential *vs.* $Ag/AgClO_4$ (0.01 M in acetonitrile–0.1 M Bu_4NPF_6). (*a*) and (*d*) **1**, (*b*) and (*e*) **5**, (*c*) and (*f*) **7**, for CVs: scan rate 50 mV s^{-1}; for DPVs: scan rate 20 mV s^{-1}, pulse amplitude 50 mV, pulse width 50 ms, pulse period 200 ms.

oxidations only in DCM [Fig. 3(*a*) for CV and 3(*d*) for DPV] leading to the dication $\mathbf{1}^{2+}$ *via* the mono-cation $\mathbf{1}^{\bullet+}$, in agreement with the chemical oxidation (for EPR measurements see below). In Py, however, the second electron-transfer is no more totally reversible, as can be seen from the smaller reduction peak [Fig. 1(*e*) for CV and 2(*e*) for DPV]. Indeed, if the second scan in pyridine is extended until −2.2 V [Fig. 4(*a*)] two small rereduction peaks a, b occur between −1.0 and −1.5 V, at potentials less negative than the above mentioned reduction couples which appear between −1.8 and −2.0 V. In the third (oxidative) scan, no reoxidation peaks corresponding to the small reduction peaks a and b can be detected. If the anodic sweep is stopped at about +0.2 V (*i.e.* after the first but before the second oxidation peak; Figure not shown), the reduction peaks a and b of the second scan do not show up any more. This means that the dication reacts with a nucleophile, presumably pyridine, in a fast reversible way, or its tetrazolium ring is cleaved into many fragments. The same CV- and DPV-responses are observed when the chemically produced and isolated cations $\mathbf{1}^{\bullet+}$ or $\mathbf{1}^{2+}$ (see above) are subjected to the electrochemical investigation. Thus, **1** was characterized as a new compound exhibiting four-step redox behaviour (Scheme 3) capable of acting both as an electron acceptor and as an electron donor, depending on the ionization potential and electron affinity of a suitable partner.[4]

The *p*-phenylene bridged species **5** undergoes also two reversible one-electron oxidations in DCM [Fig. 3(*b*) for CV, Fig. 3(*e*) for DPV]. As can be seen from Fig. 3 and Table 1, the peak-couples are less separated for **5** than for **1**; this may be a consequence of the larger distance (and hence greater independence) of the two tetrazolium rings in **5**. It further turns out that the first electron-transfer is more facile (ΔE = 197 mV)

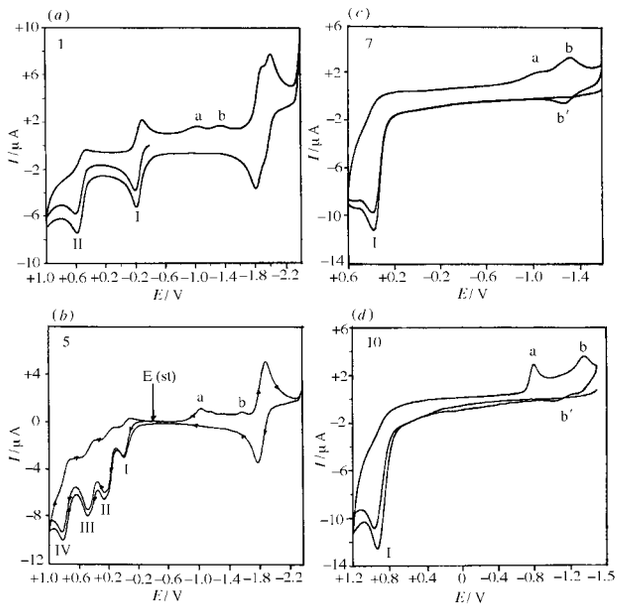

Fig. 4 Multi-sweep CVs of compounds **1**, **5**, **7** and **10** (*a*) **1** in Py, (*b*) **5** in Py, (*c*) **7** in DCM and (*d*) **10** in Py. Potential *vs.* $Ag/AgClO_4$ (0.01 M in acetonitrile–0.1 M Bu_4NPF_6), scan rate 50 mV s^{-1}.

from **1**, presumably because of the better delocalization of the odd electron over both sides in the cation radical $\mathbf{1}^{\bullet+}$ as compared to the situation with $\mathbf{5}^{\bullet+}$. The difference in the second oxidation potentials ($\Delta E = 270$ mV) is most striking. Again, the two above mentioned effects seem to be responsible: the dication $\mathbf{1}^{2+}$ apparently adopts a structure **A** of the π-system, in

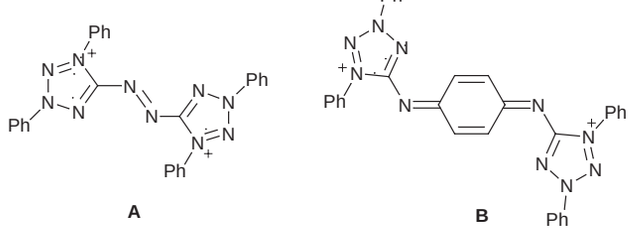

which the positive charges are localized mainly in the tetrazolium rings. This is, of course, true also for $\mathbf{5}^{2+}$, however, here the Coulomb repulsion of the two charges, the so-called "dication effect", is relieved owing to the larger distance between the tetrazolium rings (**B**), which stabilizes the dication.

In Py **5** behaves completely differently: there are apparently *four* successive quasi-reversible or irreversible oxidation peaks in the CV [Fig. 1(*f*)]. According to the DPV [Fig. 2(*f*)] it looks as if a successive four-step one-electron oxidation up to the tetracations would be possible. The number of transferred electrons as determined by coulometry, however, varies between 4.4 and 8.3, depending on the conditions. It is quite conceivable that also in Py no higher oxidation than up to the dication occurs, which then reacts with Py to give products which are further oxidized in peaks III and IV. Indeed, there are several rereduction peaks, *e.g.* those denoted by a and b, if the reverse scan is continued until −2.2 V [Fig. 4(*b*)]. The third scan does not show any reoxidation peaks of a and b (*cf.* the situation with **1**, above). If the switch potential is varied (Fig. S1, Supplementary Material), it turns out that the first oxidation peak is reversible on the time-scale of CV also in Py, and no rereduction peak a or b occurs, when the potential is reversed between the first and second oxidation peak.

The biphenylenyl compound **6**, on oxidation, gives CV and DPV curves revealing the same features as those of **5**, in Py as well as in DCM (Fig. S2 and S3, Supplementary Material). However, the peak-couples of **6** in DCM move closer together ($\Delta E = 80$ mV), which is again a consequence of the larger distance and hence stronger independence of the active tetrazolium centres in **6**. The first oxidation peak, and to a lesser degree also the second, is shifted to a more positive potential (see Table 1), which may be explained by the following arguments: In the radical cation $\mathbf{6}^{\bullet+}$ the delocalization of the odd electron is hampered by the twisting (atropisomerism) of the biphenyl system leading to a higher energy of $\mathbf{6}^{\bullet+}$ with respect to $\mathbf{5}^{\bullet+}$. Although the "dication effect" is further relieved in $\mathbf{6}^{2+}$ as compared to $\mathbf{5}^{2+}$, the biphenoquinone-bisimine structure (**C**) seems

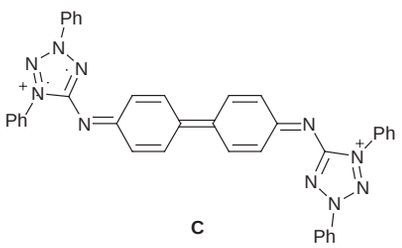

to be less stable than the quinone-bisimine structure **B**; we even have to consider an equilibrium with a biradical state of $\mathbf{6}^{2+}$.[5]

The *m*-phenylene bridged compound **7** gives rise to a CV [Fig. 1(*g*)] in Py, which shows two oxidation peaks being irreversible (I) or partially reversible (II) as well as a rereduction peak a. The DPV [Fig. 2(*g*)] confirms the two-peak oxidation. To our surprise, however, in DCM only *one* oxidation peak can be observed, which is followed by several small peaks at higher potentials, and *two* rereduction peaks a and b [Fig. 3(*c*)]. This feature with one dominant oxidation peak is also evident from the DPV [Fig. 3(*f*)]. The results indicate a slow decomposition of **7** in the oxidation process to give a complicated mixture especially in DCM. In Fig. 4(*c*) the return potential was laid close behind peak I to narrow the sweep-range in the positive part of the potential scale. As a result, the rereduction peak a in the second scan has decreased in intensity but the reduction peak b remains nearly unaffected. Therefore, the peak a must belong to a product which is formed from the oxidized species of **7** more slowly than the product which gives the rereduction peak b. In the third scan, it turns out that b has a corresponding oxidation peak b′ forming a reversible peak couple with b, whereas a shows no corresponding oxidation peak. The product X responsible for b/b′ is apparently so stable that on oxidation of **7** in peak I it is produced at or near the working electrode surface in a considerable amount. Therefore, if we do not stir the solution after CV measurement and run a DPV closely afterwards, we observe a peak at the position b′ in the positive DPV scan (not shown). We are currently endeavouring to isolate and characterize X after large scale electrolysis.

The CV features of **8** are similar to those of **7**, (Fig. S4, Supplementary Material) especially in Py, whereas in DCM only one rereduction peak a is observed. The oxidation potentials of **8** are even higher than those of **7,** which means that now an interaction between the two tetrazolium rings is practically no longer possible. And, indeed, the first oxidation potential is about the same (Table 1) as that of **9**, a mono-tetrazolium system with one phenyl ring at the exocyclic nitrogen (see below). Thus, **8** behaves like two units of **9**, arbitrarily connected by a bond.

The mono-tetrazolium compounds **9** and **10**, finally, undergo irreversible one-electron oxidations [*cf.* **10**: Fig. 1(*h*) for CV, Fig. 2(*h*) for DPV]. A three-scan multicycle CV [Py as solvent, Fig. 4(*d*)] shows two rereduction peaks a and b in the second scan, similarly to the situation with **7** in DCM. The third scan reveals that the rereduction b is partially reversible. We have to assume fragmentation of the tetrazolium part following the oxidation. The oxidation potentials of **10** are the highest in the whole series, nearly 1.2 V higher than that for **1**. In **10** there is no stabilization of the primarily formed cation-radical $\mathbf{10}^{\bullet+}$ by

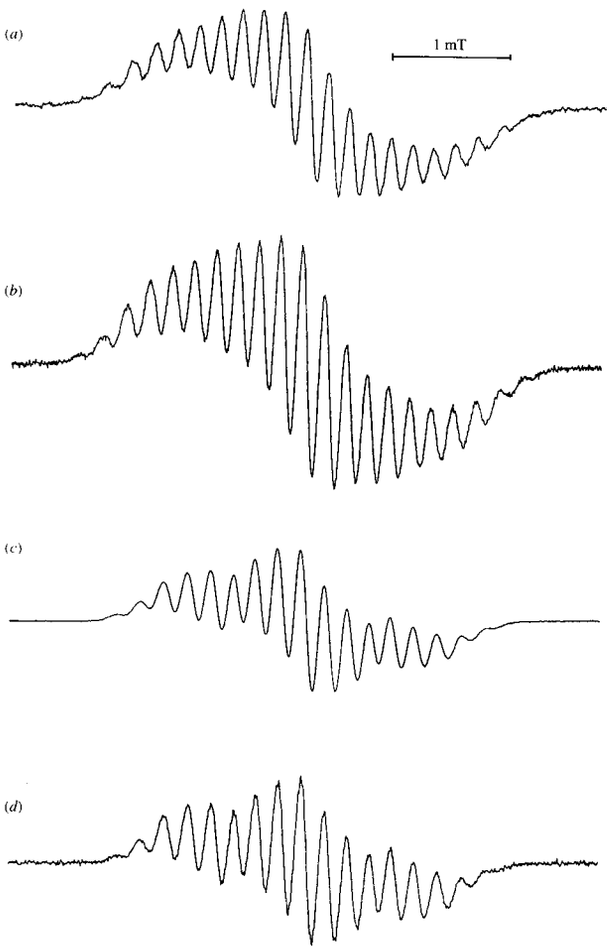

Fig. 5 EPR spectra of (*a*) $\mathbf{1}^{\bullet+}$, (*b*) $\mathbf{1a}^{\bullet+}$, (*c*) $\mathbf{1b}^{\bullet+}$ and (*d*) $\mathbf{1c}^{\bullet+}$ in DCM.

any substituent at the exocyclic nitrogen. In agreement with this neither in Py nor in DCM any reversibility can be observed. The number of electrons transferred, as determined by coulometry, is *ca.* 0.8 which points to a one-electron oxidation of **10** in the oxidation peak. However, *n*-values determined by CPE in a completely irreversible peak are surely not very accurate.

Spectroscopic and magnetic investigations

The redox processes of the tetrazolium compounds produce radical anions or cations as the primary species, which we tried to detect and characterize by UV/Vis, EPR, and ENDOR spectroscopy, and susceptibility measurements. The majority of these investigations were performed on the chemically prepared cation-radical $\mathbf{1}^{\bullet+}$, which is very stable and can easily be handled (see above). *In situ* generation by electrochemical methods was also applied in some cases.

UV Spectra. As already mentioned in the synthesis section, the radical cation $\mathbf{1}^{\bullet+}$ shows a longest-wavelength absorption (625 nm) which is bathochromic with respect to the neutral species **1**, as well as to the dication $\mathbf{1}^{2+}$, being typical for such systems.[6]

EPR Spectra of $\mathbf{1}^{\bullet+}$. Radical cation $\mathbf{1}^{\bullet+}$, generated by the electrochemical oxidation of **1** in pyridine solution at room temperature, showed the same EPR spectrum as that of the chemically prepared species $\mathbf{1}^{\bullet+}$ BF_4^- in DCM [Fig. 5(a)]; aside from the number of low-intensity lines observable at the wings of the spectrum. The *g*-value was found to be 2.00391. Both spectra are only moderately resolved, which is quite understandable because the odd electron has a chance to couple with 10 nitrogen and 20 hydrogen atoms, if it is delocalized over the whole system. Therefore, we have to expect that simulations will only give rough coupling constants. One of them with a component linewidth (ΔH) of 0.16 mT gave the hyperfine splitting constants (hfc) a_N (2) = 0.527, a_N (4) = 0.195 mT (the values in parentheses denote the number of equivalent nuclei). This means, that some of the nitrogen atoms of $\mathbf{1}^{\bullet+}$ as well as the hydrogen atoms seem to couple only insignificantly with the free electron. As judged from the molecular structure we should expect a detachment of the electron on oxidation of **1** from the exocyclic nitrogen atom N_{exo}. The free spin density should therefore be highest and the hfc largest for N_{exo} (resonance structure **D**). *Via* allylic resonance, spin density should also be transferred to N-4 (resonance structure **E**). The moiety Ph–

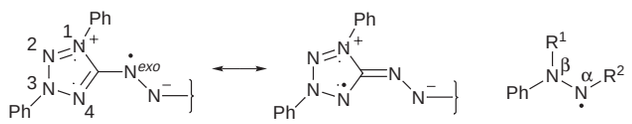

D **E** **F**

(N-3)–(N-4) in **E** corresponds to the fragment **F** present in linear (DPPH) or cyclic hydrazyls (verdazyls, tetrazolyls). These compounds develop a free spin density also at the adjacent N_β atom, being nearly as large as that on N_α,[7] whereas the coupling with the hydrogen atoms of the phenyl ring is small and about the same for *ortho*- and *para*-protons.[7] By analogy, two hfc's a_N (2) (N_{exo}) and a_N (4) (N-3, N-4) would be reasonable for $\mathbf{1}^{\bullet+}$, implying that the electron is equally distributed over equivalent positions in both moieties of the molecule.

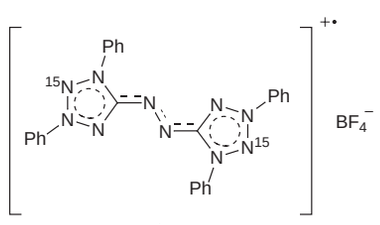

$\mathbf{1a}^{+\bullet}$

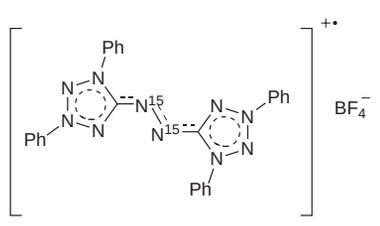

$\mathbf{1b}^{+\bullet}$

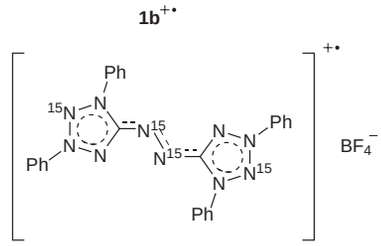

$\mathbf{1c}^{+\bullet}$

In order to facilitate a determination of the nitrogen couplings *experimentally*, we prepared three types of ^{15}N-labelled analogues ($\mathbf{1}^{\bullet+}$**a**–**c**) of $\mathbf{1}^{\bullet+}$ with ^{15}N atoms in the positions shown in the respective formulae. Their EPR spectra in DCM [Fig. 5(b)–(d), respectively] reveal an interesting phenomenon: The spectrum of $\mathbf{1a}^{\bullet+}$ (^{15}N in positions 2 and 2′) does not show any change as compared to that of $\mathbf{1}^{\bullet+}$, whereas the spectrum of $\mathbf{1b}^{\bullet+}$ (^{15}N in both N_{exo} positions) is distinctly different. The spectrum of the tetra-labelled species $\mathbf{1c}^{\bullet+}$ (^{15}N in 2-, 2′- and both *exo*-positions), as expected from the just described

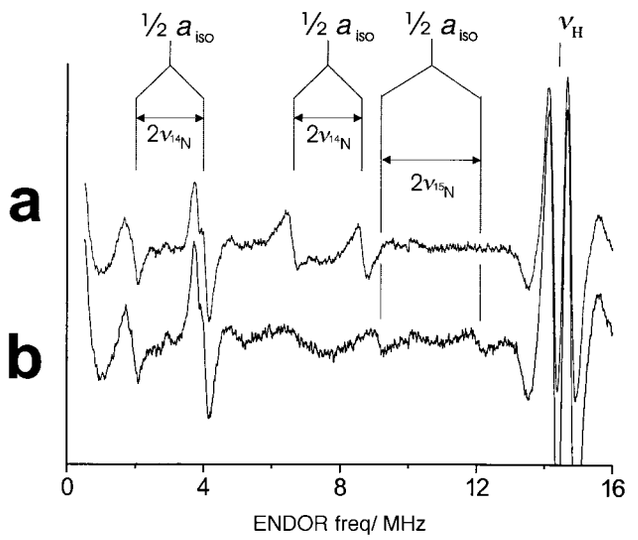

Fig. 6 ENDOR spectra of (a) **1a**$^{\bullet+}$ and (b) **1b**$^{\bullet+}$. The spectrum of **1**$^{\bullet+}$ (not shown) is similar to (a). Nitrogen ENDOR lines are centred about $1/2a_{iso}$, the isotropic hfc, and spaced by $2\nu_n$, the Larmor frequency of the free nucleus (^{14}N, ^{15}N or H). Experimental conditions: solvent: DCM; P_{rf} (radiofrequency power): 30 W, P_{mw} (microwave power): 24 mW, rf frequency modulation: 30 kHz, with 100 kHz deviation, broad baseline features were subtracted. (a): Temperature $T = 280$ K, 45 min total measuring time; (b): $T = 270$ K, 34 min.

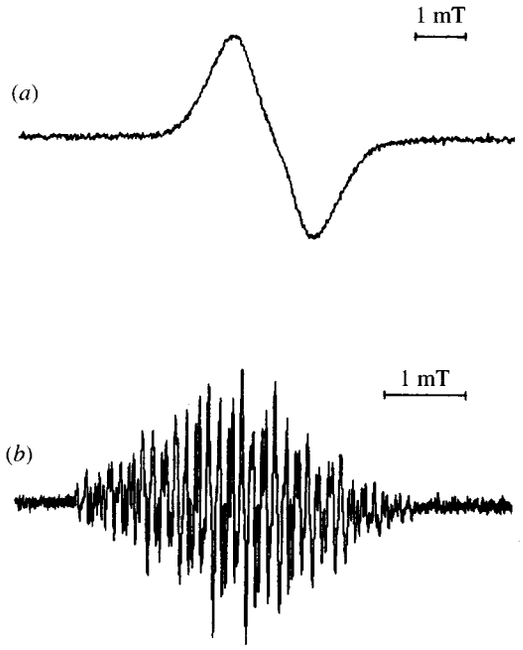

Fig. 7 EPR spectra obtained on cathodic reduction of (*a*) **1** and (*b*) **10** in Py.

features of **1a**$^{\bullet+}$ and **1b**$^{\bullet+}$, completely coincides with that of **1b**$^{\bullet+}$. As a consequence, a coupling of the free electron with N-2 and N-2′ cannot be detected, *i.e.* $a_{N\text{-}2}$ and $a_{N\text{-}2'}$ should be smaller than the line-width (<0.09 mT). The EPR spectra of **1b**$^{\bullet+}$ (and **1c**$^{\bullet+}$), on a first order treatment, show a large triplet structure (1:2:1) with each triplet line being further split into a nonet [the multiplicity is close to the theoretical one (1:4:10:16:19:16:10:4:1)], the three nonets being partially overlapped. The triplet splitting results from two equivalent ^{15}N-nuclei, the nonet splitting from four equivalent ^{14}N-nuclei. The *a*-values, directly extracted from the EPR spectrum of **1b**$^{\bullet+}$ are: $a_{^{15}N}$ (2) = 0.75 mT and $a_{^{14}N}$ (4) = 0.185 mT. The value of $a_{^{15}N}$ (2) corresponds to $a_{^{14}N}$ (2) = 0.53 mT in **1**$^{\bullet+}$ ($a_{^{14}N} = a_{^{15}N} \times$ 0.7129 from the gyromagnetic ratio). The results agree well with the simulation of the spectrum of **1**$^{\bullet+}$ mentioned above and prove (i) that the largest hfc belongs to N_{exo}, (ii) that both N_{exo} are equivalent, *i.e.* the free electron is symmetrically delocalized over both moieties of the molecule. In conformity with earlier considerations (see above), the smaller $a_{^{14}N}$-value should be attributed to N-3, N-3′, N-4 and N-4′. Strictly speaking, $a_{N\text{-}3}$ and $a_{N\text{-}4}$ are not exactly equivalent and, indeed, a refined simulation ($\Delta H = 0.0837$ mT) of the spectrum of **1**$^{\bullet+}$ (S5, Supplementary Material) reveals two inequivalent ^{14}N-couplings, *i.e.* 0.185 and 0.199 mT, besides $a_{^{14}N} = 0.530$ mT. Presumably, the larger one (0.199 mT) belongs to N-3 and N-3′, the smaller one (0.185 mT) to N-4 and N-4′, quite in analogy to the results obtained with DPPH, verdazyls and tetrazolyls.[7]

ENDOR Spectra. These results were confirmed by ENDOR experiments (Fig. 6). Two ^{14}N hfc's were observed for **1a**$^{\bullet+}$: $a_1 = 15.1$ MHz (0.539 mT) and $a_2 = 5.9$ MHz (0.21 mT). The larger hfc a_1 can again unambiguously be assigned to the exocyclic nitrogens by comparison with the selectively ^{15}N labelled compound **1b**$^{\bullet+}$, because in the ENDOR spectra of **1b**$^{\bullet+}$ the lines due to a_1 in **1a**$^{\bullet+}$ are absent. Instead, two lines corresponding to $a = 21.2$ MHz (0.756 mT) are observed, as expected. The ENDOR lineshapes for the lines corresponding to a_2 show a small splitting, indicating that two inequivalent groups of nitrogens contribute, one with $a_{2a} = 5.6$ MHz (0.198 mT), the other with $a_{2b} = 6.0$ MHz (0.214 mT). Comparison with **1c**$^{\bullet+}$ reveals no changes in the position and in the shape of these lines. Furthermore, no additional lines are observed, in particular not in the frequency region where ENDOR resonances would be expected if any of the ^{14}N nuclei contributing to a_2 were replaced by ^{15}N. This again suggests that the hfc of ^{15}N-2 in **1c**$^{\bullet+}$ does not contribute to a_2, and that the hfc of the nitrogens at that position was too small to be observed by ENDOR ($a < 1.5$ MHz; 0.05 mT).§ Proton ENDOR lines (0.50 MHz; 0.018 mT) were observed in the region around ν_H, the Larmor frequency of the free proton, which are assigned to the only protons in the radical, *i.e.* those of the phenyl rings. No attempt was made to resolve the hfc's expected for the different protons of the phenyl rings.

EPR Spectra on cathodic reductions. The EPR spectrum obtained on cathodic reduction of **1** is shown in Fig. 7(*a*). Contrary to the radical-cation **1**$^{\bullet+}$ only a broad line could be observed; the *g*-value was 2.00294. The poor resolution might result from an interaction of the odd electron with all ten nitrogen nuclei in a radical-anion **1**$^{\bullet-}$. However, since the two reduction potentials of **1** lie close together, and a potential control was not possible in our *intra-muros* electrochemical cell, a reduction to the dianion **1**$^{2-}$ might have occurred. Contrary to the dication **1**$^{2+}$ (see below), this dianion could well be in equilibrium with a diradical whose dipolar coupling would then be responsible for the bad resolution. This possibility is currently being tested.

Compound **10**, however, can be reduced electrochemically by one-electron transfer to a radical anion **10**$^{\bullet-}$. We observed an EPR spectrum [Fig. 7(*b*)] with $g = 2.00397$. The resolution is much better than in all other cases discussed in this paper. Unfortunately, all attempts to simulate it in terms of the ^{14}N and ^{1}H nuclei of **10**$^{\bullet-}$ failed. Therefore, the EPR spectrum could belong to a mixture of **10**$^{\bullet-}$ and a cleavage product therefrom, the more so, since the analogue **9** could be cleaved by reduction with zinc (see above). Unfortunately, these radical anions are not persistent enough for the ENDOR measurement

§ Although this is a plausible suggestion, which qualitatively agrees with the results of the simulation of the EPR spectra, the difficulties associated with ENDOR at these low frequencies (see Experimental section), which are compounded by the unfavourable relaxation properties of nuclei like ^{14}N and ^{15}N in solution, limits the degree of confidence in arguments based on the absence of ENDOR signals.

to get a final proof for their structure and further insight into the odd electron distribution.

Susceptibility measurements. The dication $\mathbf{1}^{2+}$ is diamagnetic and no triplet system, as can be seen from its well-resolved NMR spectrum and the temperature-independent magnetic susceptibility (-2.4×10^{-4} emu mol^{-1}) observed in a SQUID magnetometer for a powdered sample, if care is taken that no monocation $\mathbf{1}^{\bullet+}$ is present as impurity. The monocation $\mathbf{1}^{\bullet+}$, on the other hand, reveals temperature-dependent paramagnetism (*ca.* 1.42 Bohr magnetons without diamagnetic correction) with a normal Curie–Weiss behaviour between 50–300 K. At lower temperature, there is a deviation to higher magnetic moments, which is not yet understood.

Conclusions and summary

A series of mesoionic compounds **1** and **5**–**10** are now easily accessible, even in the solid state. These compounds are very stable and can be oxidized or reduced chemically or electrochemically; in some cases the processes are reversible and occur stepwise *via* ion-radicals to diions (cations and anions). It turned out that, in general, the oxidation products are more stable in DCM, the reduction products in Py. This is reasonable because DCM is a weak electrophile reacting with anions, whereas Py acts as a strong nucleophile, attacking cations. Aside from these solvent effects, the stability of the substrate ions seems to be favoured largely by two effects: (i) a strong delocalization of the free electron in the ion-radical with a preferential residence on the exocyclic link atoms, thus allowing for a more or less localization of the charges in the tetrazolium rings, (ii) a π-conjugation of the ionic centres in the diions, which tends to separate the charges as far as possible. Both effects will be strongly influenced by the distance of the tetrazolium rings. The larger the distance, the less the Coulomb repulsion between the charges (diion effect)—but also the delocalization of the free electron is less effective.

The effects (i) and (ii) are well demonstrated in the case of **1** which is the most thoroughly investigated species of the present series. It can be oxidized stepwise to the cation-radical $\mathbf{1}^{\bullet+}$ and the dication $\mathbf{1}^{2+}$, both of which could be isolated as stable BF_4^- salts. A comprehensive EPR/ENDOR study, using also specific ^{15}N-labelling, shows that in the cation-radical $\mathbf{1}^{\bullet+}$, indeed, the free electron is delocalized over both moieties of the molecule, although not uniformly over all N-atoms of the tetrazolium ring; only two ring N-atoms reveal a detectable coupling and hence indicate a free spin density at the corresponding ring positions.¶ In the sense of the above statement (i), however, the predominant part of the free spin density is experimentally found at the two exocyclic (hydrazo) nitrogens. This may, therefore, be the reason for the stability and the very low first oxidation potential of **1**. The likewise remarkable stability of the diamagnetic dication $\mathbf{1}^{2+}$, on the other hand, may be a consequence of (ii), *i.e.* the formation of an azo-bridge between the tetrazolium cationic centres.

In the case of **5**–**10**, we note a fundamental difference between the *para*-bridged bis-tetrazolium systems **5** and **6** on the one hand and the *meta*-bridged species **7** and **8** on the other. On oxidation, the first mentioned molecules produce cation-radicals ($\mathbf{5}^{\bullet+}$, $\mathbf{6}^{\bullet+}$) and dications ($\mathbf{5}^{2+}$, $\mathbf{6}^{2+}$) successively, which are stabilized by resonance ($\mathbf{5}^{\bullet+}$, $\mathbf{6}^{\bullet+}$) or by formation of a conjugated quinonoid system ($\mathbf{5}^{2+}$, $\mathbf{6}^{2+}$). The difference in Py and DCM as solvents results only from the ability of Py to exert a nucleophilic attack on $\mathbf{5}^{\bullet+}$, $\mathbf{6}^{\bullet+}$ and, especially, on $\mathbf{5}^{2+}$, $\mathbf{6}^{2+}$. Since the positive charges in the dications $\mathbf{5}^{2+}$ and $\mathbf{6}^{2+}$ are far more separated than in $\mathbf{1}^{2+}$, the second oxidation potentials of **5** and **6** are much lower than that of **1**. The *meta*-bridged species, on the other hand, give cation-radicals $\mathbf{7}^{\bullet+}$, $\mathbf{8}^{\bullet+}$ and dications (presumably existing as diradicals) $\mathbf{7}^{2+}$, $\mathbf{8}^{2+}$ which are much less stabilized, because the *meta*-junction, aside from an additional degree of twisting, neither allows a delocalization of the odd electron in $\mathbf{7}^{\bullet+}$, $\mathbf{8}^{\bullet+}$ over the whole system in terms of canonical structures nor a conjugated quinonoid π-system in $\mathbf{7}^{2+}$, $\mathbf{8}^{2+}$. This is nicely reflected by the higher oxidation (peak) potentials of **7** and **8** relative to those of **5** and **6** and the small variation of these values between Py and DCM as solvents. The instability of the oxidized species of **7** and **8** is thus an intrinsic one and not caused by the nucleophilic attack of Py; therefore, DCM does not give any advantage over Py as solvent in the oxidation of these species.

In the case of reduction, the formation of the anion-radicals and dianions occurs at very similar potentials, which either means that the anion-radical state is more difficult or the dianion state more easy to reach from the neutral state as compared to the corresponding cationic species. Since the potentials correspond to those of the monovalent reduction of the monotetrazolium systems **9** and **10**, the first suggestion seems to be true, which means that resonance stabilization of the anion-radicals should be less effective than that of the cation-radicals; unfortunately, the EPR spectra obtained on reduction of **1** and **10** do not give any information hereto. At the same time, the dianions might exist as diamagnetic conjugated species or as diradicals with negligible interaction behaving like two separate mono-radicals. This would explain why the potential of the second electron transfer is about the same as that of the first one and why for all compounds **1**, **5**–**10** the reduction potentials do not vary appreciably. Altogether, the mesoionic species presented here show several interesting features,[5] which could be of importance for materials science, whose understanding however requires further investigations.

Experimental

General

Melting points were measured with a hot-stage apparatus and are uncorrected. Elemental analyses were carried out at the Elemental Analysis Centre of Kyoto University. IR spectra were taken as KBr discs on a JASCO A-102 spectrometer. Electronic spectra were measured on a Hitachi 124 or U-3500 spectrophotometer. NMR spectra were obtained using a Hitachi 90 (90 MHz for ^{1}H), a Varian XL-200, Varian Gemini 200 (200 MHz and 50 MHz, for ^{1}H and ^{13}C, respectively) or a Bruker AMX 400 (400 MHz and 100 MHz, for ^{1}H and ^{13}C, respectively). Chemical shifts are recorded in ppm downfield from tetramethylsilane. *J* values are given in Hz. Assignment of signals was made based on the chemical shifts, peak intensities and INEPT techniques. Mass spectra were taken with a Hitachi M-2000S spectrometer (EI, 70 eV). SQUID measurements were carried out with a Quantum Design, MPMS system.

^{15}N-sodium nitrite (99% ^{15}N) and $^{15}N_2$-hydrazine sulfate (99% ^{15}N) were purchased from Isotec Inc.

Although no problems were encountered, it should be noted that polyaza compounds as well as the perchlorates used for the electrochemical procedures in general may be explosive and should be handled with due care.

Electrochemical and EPR/ENDOR measurements

Electrochemical experiments were carried out on a Windows-driven BAS 50W electrochemical analyzer (Bioanalytical Systems, Inc., West Lafayette, IN 47906, USA). For CV and DPV a 3 mm platinum or glassy carbon electrode (Metrohm) was used as working electrode. The auxiliary electrode consisted of a Pt wire or disk. $Ag/AgClO_4$ (0.01 M in MeCN/0.1 M Bu_4NPF_6) was used as reference electrode and all potentials given relate to this electrode. The formal potentials of the ferrocene/ferrocenium electrode against this reference electrode

¶ Therefore, strictly speaking, the ring symbols in the tetrazolium rings used in the formulae $\mathbf{1a}^{\bullet+}$, $\mathbf{1b}^{\bullet+}$ and $\mathbf{1c}^{\bullet+}$ are only of a formal nature.

are 0.19 and 0.21 V in Py and DCM solutions, respectively. It was separated by two glass frits from the Haber-Luggin capillary. The compartment between reference electrode and H.-L. capillary was filled with 0.1 M Bu_4NPF_6–acetonitrile solution. The H.-L. capillary itself always contained the same solution as the cell for the measurements. For CPE cylindrical Pt (10% iridium) gauze working and auxiliary electrodes, separated by two porous glass frits, were used. To the compartment containing the auxiliary electrode, quinhydrone in 10-fold excess over the investigated compound was added to ease the electron transfer. High quality commercial pyridine (Fluka) stored over 4 Å molecular sieves was used without further treatment. Alternatively, commercial pyridine was purified by distilling it three times under argon after drying over KOH for several weeks, and then kept over 4 Å molecular sieves. DCM was refluxed over P_2O_5 for several hours and afterwards distilled twice. Tetrabutylammonium hexafluorophosphate (Bu_4NPF_6) as supporting electrolyte was prepared from tetrabutylammonium bromide and ammonium hexafluorophosphate or purchased (Fluka), recrystallised four times from EtOH and dried *in vacuo* at 110 °C for 48 h. The concentration of the substrates was 0.3–2 mM.

EPR spectra were obtained with a Bruker ESP 300E spectrometer. For *g*-factor measurements, the field gradients were corrected by replacing the sample with a reference compound (2,6-di-*tert*-butyl-4-*tert*-butoxyphenoxyl in benzene, $g = 2.00463$). All ENDOR spectra were measured with a laboratory developed spectrometer described elsewhere[8] on samples prepared on a high vacuum line, by dissolving the solid radical in DCM, and degassed by repeated freeze–pump–thaw cycles. DCM was dried over calcium hydride. As baseline artifacts due to cross talking of microwave (mw) and radio-frequency (rf) fields are common in the low frequency region of the ENDOR spectrum, and since the partially resolved EPR spectrum of the sample causes baseline artifacts which can appear as lines, the following control experiments were performed to discriminate artifacts from ENDOR lines: by changing the magnitude of the static magnetic field B_0 and employing B_0 modulation, lines due to cross talking of mw and rf fields should shift or be suppressed, thus ENDOR signals were identified by not being susceptible to these changes. The temperature dependence of the relaxation rates governing liquid solution ENDOR intensities[9] causes pronounced intensity changes of ENDOR lines with temperature, which is not the case for the spurious background signals. Thus, the ENDOR signals were further identified by having temperature dependent intensities.

Synthesis

5,5′-Azinobis(1,3-diphenyltetrazole) (1). A mixture of 5-chloro-1,3-diphenyltetrazolium tetrafluoroborate[3] (0.35 g, 1.0 mmol) and hydrazine hydrate (80%, 0.32 ml, 5.0 mmol) in acetonitrile (50 ml) was stirred at room temperature for 2 h. The solvent was evaporated and the residue dissolved in DCM. Insoluble materials were filtered off and the filtrate was evaporated to dryness. The residual solid was recrystallised from DCM–ether to give **1** as deep purple crystals (0.17 g, 72%); mp > 300 °C (Found: C, 66.2; H, 4.2; N, 29.8. Calc. for $C_{26}H_{20}N_{10}$: C, 66.1; H, 4.3; N, 29.65%); ν_{max}/cm^{-1} 3090, 1614, 1580, 1490, 1470, 1372, 1322, 1290, 1214, 1156, 1070, 970, 760, 700 and 692; λ_{max} (DCM)/nm 269 (sh, log ε 4.64), 280 (4.65) and 542 (3.73); δ_H (90 MHz; $CDCl_3$) 7.12–7.76 (12H, m, Ph) and 7.94–8.40 (8H, m, Ph); δ_C (50 MHz; $CDCl_3$) 120.4 (C-*o*), 120.9 (C-*o*), 127.1 (C-*m*), 129.7 (C-*p*), 129.9 (C-*p*), 131.5 (C-*m*), 136.5 (C-*i*), 136.9 (C-*i*) and 158.4 (C^+); *m*/*z* 472 (M^+, 100%).

Methylation of 1. To a solution of azine **1** (60 mg, 0.13 mmol) in DCM (10 ml) was added methyl iodide (0.34 g, 2.4 mmol), and the mixture was refluxed for 12 h. An additional amount of methyl iodide (0.34 g, 2.4 mmol) was added and the mixture was further refluxed for 3 h. $NaBF_4$ (1.0 g) in water (10 ml) was added and the organic layer was separated, dried (Na_2SO_4), and evaporated. The residue was chromatographed on silica gel (DCM–acetone = 1 : 1) to give **2** as brass-yellow crystals (41 mg, 56%); mp 221–222 °C (from EtOH) (Found: C, 56.4; H, 4.2; N, 24.2. Calc. for $C_{27}H_{23}BF_4N_{10}$: C, 56.5; H, 4.0; N, 24.4%); ν_{max}/cm^{-1} 1658, 1606, 1580, 1492, 1472, 1462, 1378, 1340, 1300, 1284, 1222, 1180, 1060, 990, 774 and 688; δ_H (90 MHz; $CDCl_3$) 3.64 (3H, s, Me), 7.00–7.78 (16H, m, Ph) and 7.98–8.32 (4H, m, Ph); δ_C (50 MHz; $CDCl_3$) 40.2 (Me), 120.9 (C-*o*), 121.5 (two overlapped signals) (C-*o*), 126.6 (C-*o*), 129.1 (C-*m*), 129.4 (C-*p*), 129.7 (C-*m*), 130.6 (two overlapped signals) (C-*m*), 131.6 (C-*p*), 132.8 (C-*p*), 133.6 (C-*p*), 133.8 (C-*i*), 134.2 (C-*i*), 135.7 (C-*i*), 135.8 (C-*i*), 157.8 (C^+) and 163.4 (C^+).

Protonation of 1. Azine **1** (60 mg, 0.13 mmol) was dissolved in DCM (15 ml) and acetic acid (50 µl) was added. The mixture was stirred for 5 min and poured into aqueous sodium tetrafluoroborate (2.7 g in 30 ml of water). The organic layer was separated, dried (Na_2SO_4), and the solvent was evaporated to give monoprotonated compound **3** (63 mg, 85%) as brownish orange crystals; mp 130 °C (from EtOH–hexane) (Found: C, 55.1; H, 4.0; N, 24.3. Calc. for $C_{26}H_{21}BF_4N_{10}\cdot 0.5H_2O$: C, 54.9; H, 3.9; N, 24.6%); ν_{max}/cm^{-1} 3345, 3040, 1696, 1614, 1586, 1490, 1460, 1380, 1338, 1292, 1234, 1196, 1060, 984, 924, 772 and 688; δ_H (200 MHz; $CDCl_3$) 7.62 (12H, br m, Ph) and 8.25 (8H, br m, Ph).

Diprotonated compound (4). Azine **1** (44 mg, 0.093 mmol) was dissolved in trifluoroacetic acid (0.50 ml) to give a colourless solution. Excess trifluoroacetic acid was evaporated to dryness to give colourless crystals of **4** in quantitative yield. An analytical sample was dried under vacuum at 50 °C (Found: C, 41.9; H, 2.4; N, 13.6. Calc. for $C_{30}H_{22}F_6N_{10}O_4\cdot 3(CF_3CO_2H)$: C, 41.5; H, 2.4; N, 13.4%); ν_{max}/cm^{-1} 3105, 2900, 1780, 1652, 1626, 1496, 1464, 1436, 1376, 1324, 1298, 1212, 1170, 1142, 998, 928, 842, 818, 800, 786, 766, 730, 712, 702 and 680; δ_H (90 MHz; CF_3CO_2D) 7.45–7.85 (16H, m, Ph) and 7.90–8.24 (4H, m, Ph); δ_C (50 MHz; CF_3CO_2D) 122.5 (C-*o*), 126.5 (C-*o*), 132.3 (C-*i*), 132.6 (C-*m*), 133.2 (C-*m*), 135.9 (C-*p*), 136.5 (C-*p*), 136.8 (C-*i*) and 159.9 (C^+).

Oxidation of 1: Synthesis of radical cation ($1^{\bullet+}$). To a solution of **1** (0.47 g, 1.0 mmol) in DCM (20 ml) was added lead tetraacetate (0.25 g, 0.50 mmol), and the mixture was stirred at room temperature for 10 min. $NaBF_4$ (1.0 g) in water (10 ml) was added and the organic layer was separated. The layer was washed with $NaHCO_3$ (5%) and the solvent was evaporated under vacuum. The residue was column-chromatographed on silica gel (DCM–acetone = 4 : 1) to give $\mathbf{1}^{\bullet+}$ as greenish brown crystals (0.17 g, 31%); mp 185–189 °C (from MeOH–Et_2O) (Found: C, 55.7; H, 3.3; N, 24.75. Calc. for $C_{26}H_{20}BF_4N_{10}$: C, 55.8; H, 3.6; N, 25.0%); ν_{max}/cm^{-1} 1592, 1492, 1450, 1358, 1210, 1054, 986, 762 and 670; λ_{max} (MeCN)/nm 297 (log ε 4.58), 350 (sh, 4.29), 448 (4.03) and 625 (sh, 3.46).

^{15}N-labelled analogues ($1^{\bullet+}$a–c). The labelled compounds $\mathbf{1}^{\bullet+}$**a**–**c** were synthesized by the oxidation of **1a**–**c**. Compound **1a** was prepared from 2-^{15}N-5-chloro-1,3-diphenyltetrazolium tetrafluoroborate, which was synthesized according to the published method[3,10] by using ^{15}N-sodium nitrite. Compound **1b** was obtained by the condensation of 5-chloro-1,3-diphenyltetrazolium tetrafluoroborate with $^{15}N_2$-hydrazine sulfate: To a mixture of 5-chloro-1,3-diphenyltetrazolium tetrafluoroborate (0.70 g, 2.0 mmol) and $^{15}N_2$-hydrazine sulfate (0.13 g, 1.0 mmol) in acetonitrile (100 ml) was added dropwise aqueous NaOH (1 M, 20 ml). The mixture was stirred for 10 min. The resulting precipitate was filtered, washed with water, and dried to give **1b** (0.25 g, 52%). In the same manner, **1c** was obtained from

2-^{15}N-5-chloro-1,3-diphenyltetrazolium tetrafluoroborate and $^{15}N_2$-hydrazine sulfate.

Dication (1^{2+}). Crystals of **1** (0.30 g, 0.63 mmol) were added in portions to concentrated nitric acid (10 ml), and the mixture was stirred for 10 min. $NaBF_4$ (11 g) in water (20 ml) was added and the resulting orange crystals were filtered, washed with water, and dried to give $\mathbf{1}^{2+}$ (0.36 g, 87%); mp 193–196 °C (Found: C, 48.3; H, 3.2; N, 21.85. Calc. for $C_{26}H_{20}B_2F_8N_{10}$: C, 48.3; H, 3.1; N, 21.7%); ν_{max}/cm^{-1} 1492, 1460, 1374, 1308, 1290, 1246, 1180, 1060, 1000, 926, 786, 770, 710, 696 and 684; λ_{max} (MeCN)/nm 293 (log ε 4.49), 352 (sh, 4.15) and 446 (3.88); δ_H (90 MHz; CF_3CO_2D) 7.76–8.14 (12H, m, Ph), 8.14–8.36 (4H, m, Ph) and 8.36–8.70 (4H, m, Ph); δ_C (50 MHz, CF_3CO_2D) 123.5 (C-*o*), 127.6 (C-*o*), 132.9 (C-*m*), 133.0 (C-*m*), 133.3 (C-*i*), 136.6 (C-*p*), 137.4 (C-*p*), 137.1 (C-*i*) and 161.8 (C^+).

Oxidation of radical cation $1^{\cdot+}$ to dication 1^{2+}. Radical cation $\mathbf{1}^{\cdot+}\cdot BF_4^-$ (26 mg, 0.047 mmol) was added to concentrated nitric acid (0.50 ml). The mixture was ultrasonicated for 5 min and worked up as above to give $\mathbf{1}^{2+}$ (29 mg, 95%).

Reduction of radical cation $1^{\cdot+}$ to azine 1. A mixture of radical cation $\mathbf{1}^{\cdot+}$ (39 mg, 0.070 mmol) and zinc powder (14 mg, 0.21 mmol) in acetonitrile (10 ml) was stirred for 10 min under argon. The solvent was removed under reduced pressure and the residue was dissolved in DCM. The mixture was shaken with aqueous $NaHCO_3$ (5%). The organic layer was separated, dried (Na_2SO_4), and evaporated. The residue was column-chromatographed on silica gel (DCM–acetone = 4 : 1) to give **1** (25 mg, 76%).

Reduction of dication 1^{2+} to azine 1. A mixture of dication $\mathbf{1}^{2+}$ (42 mg, 0.065 mmol) and zinc powder (71 mg, 1.1 mmol) in acetonitrile (20 ml) was stirred for 20 h. The solvent was removed under reduced pressure and the residue was dissolved in DCM. The solution was shaken with aqueous $NaHCO_3$ (5%). The organic layer was separated, dried (Na_2SO_4), and evaporated. The residue was column-chromatographed on alumina (DCM–acetone = 4 : 1) to give **1** (20 mg, 65%).

Reduction of dication 1^{2+} to radical cation $1^{\cdot+}$. A suspension of dication $\mathbf{1}^{2+}$ (50 mg, 0.077 mmol) in ethanol (50 ml) was stirred at room temperature for 24 h. The reaction mixture turned from orange to greenish brown, and the crystals of $\mathbf{1}^{2+}$ gradually went into solution. The solvent was evaporated and the residue was chromatographed on silica gel (DCM–acetone) to give $\mathbf{1}^{\cdot+}\cdot BF_4^-$ (21 mg, 49%).

***N*,*N*′-Bis(1,3-diphenyltetrazolium-5-yl)-*p*-phenylenediamide (5).** A mixture of 5-chloro-1,3-diphenyltetrazolium tetrafluoroborate (2.0 g, 5.8 mmol) and *p*-phenylenediamine (0.65 g, 6.0 mmol) in acetonitrile (17 ml) was stirred at room temperature for 24 h. Water was added and the resulting precipitate was filtered, washed with water, and dried to give crystals of the conjugate acid (1.5 g, 70%); mp 260–262 °C. The acid (2.1 g, 2.9 mmol) was dissolved in acetonitrile (29 ml) and aqueous NaOH (1 M, 87 ml) was added. A reddish-purple precipitate was formed immediately, which was filtered, washed with water, and dried to give *N*,*N*′-bis(1,3-diphenyltetrazolium-5-yl)-*p*-phenylenediamide (1.6 g, 100%); mp 284–286 °C (Found: C, 69.2; H, 4.4; N, 25.3. Calc. for $C_{32}H_{24}N_{10}\cdot 0.5H_2O$: C, 68.9; H, 4.5; N, 25.1%); ν_{max}/cm^{-1} 1614, 1590, 1484, 1464, 1368, 1322, 1288, 1252, 1196, 1170, 1148, 1112, 1090, 1064, 962, 750, 698 and 678; λ_{max} ($CHCl_3$)/nm 296 (log ε 4.96), 370 (sh, 4.04) and 443 (sh, 3.64); δ_H (200 MHz; $CDCl_3$) 7.26 (4H, s, ArH), 7.39 (2H, t, *J* 8, Ph), 7.48–7.64 (10H, m, Ph), 8.21 (4H, m, Ph) and 8.43 (4H, br d, *J* 8, Ph); *m*/*z* 548 (M^+, 100%), 105 (PhN_2, 15) and 77 (Ph, 18).

***N*,*N*′-Bis(1,3-diphenyltetrazolium-5-yl)biphenyl-4,4′-diamide (6).** A mixture of 5-chloro-1,3-diphenyltetrazolium tetrafluoroborate (0.35 g, 1.0 mmol) and benzidine (0.18 g, 1.0 mmol) in acetonitrile (3.0 ml) was stirred at room temperature for 24 h. Water was added and the resulting precipitate was filtered and washed with water. The product was suspended in DCM (30 ml) and aqueous NaOH (1 M, 10 ml) was added. The mixture was vigorously stirred and the red DCM layer was separated, dried over anhydrous sodium sulfate, and evaporated. A dark-red solid (0.25 g, 79%) was obtained, which was recrystallised from DCM (*ca.* 15 ml) to give the pure product (0.18 g, 55%); mp > 300 °C (Found: C, 72.5; H, 4.6; N, 22.2. Calc. for $C_{38}H_{28}N_{10}\cdot 0.5H_2O$: C, 72.0; H, 4.6; N, 22.1%); ν_{max}/cm^{-1} 1620, 1580, 1488, 1370, 1334, 1286, 1254, 1210, 1174, 1110, 1070, 962, 826, 756, 680; λ_{max} ($CHCl_3$)/nm 296 (log ε 4.46) and 376 (sh, 3.18); δ_H (200 MHz; $CDCl_3$) 7.42 (2H, t, *J* 8), 7.48–7.70 (18H, m), 8.22 (4H, m) and 8.40 (4H, br d, *J* 8); δ_C (100 MHz, $CDCl_3$) 120.2, 121.3, 122.9 (C-*o* and C-Ar); 126.7 (C-Ar), 127.9 (C-*p*), 129.1 (C-*m*), 129.6 (C-*m*), 131.2 (C-*p*); 134.0, 135.3, 136.4 (C-*i* and Cq-Ar); 147.4 (Ar-C-N) and 154.3 (C^+); *m*/*z* (FD) 624 (M^+).

***N*,*N*′-Bis(1,3-diphenyltetrazolium-5-yl)-*m*-phenylenediamide (7).** A mixture of 5-chloro-1,3-diphenyltetrazolium tetrafluoroborate (0.41 g, 1.2 mmol) and *m*-phenylenediamine (0.13 g, 1.2 mmol) in acetonitrile (3.0 ml) was stirred at room temperature for 24 h. Water was added and the resulting precipitate was filtered, washed with water, and dried to give crystals of the conjugate acid (0.22 g, 51%); mp 112–120 °C. The acid (0.13 g, 0.18 mmol) was dissolved in acetonitrile (2.0 ml) and aqueous NaOH (1 M, 6.0 ml) was added. A reddish-purple precipitate was formed immediately, which was filtered, washed with water, and dried to give *N*,*N*′-bis(1,3-diphenyltetrazolium-5-yl)-*m*-phenylenediamide (89 mg, 92%); recrystallisation from ethanol gave a pure sample (28 mg, 27%); mp 83 °C (Found: C, 66.3; H, 4.25; N, 24.1. Calc. for $C_{32}H_{24}N_{10}\cdot 1.5H_2O$: C, 66.8; H, 4.7; N, 24.3%); ν_{max}/cm^{-1} 1620, 1556, 1484, 1466, 1364, 1322, 1278, 1238, 1202, 1148, 1104, 1064, 952, 904, 872, 816, 750 and 678; λ_{max} ($CHCl_3$)/nm 272 (log ε 4.50) and 448 (sh, 3.20); δ_H (200 MHz; [$^2H_6$]DMSO) 6.93 (2H, d, *J* 8), 7.10 (1H, t, *J* 8), 7.46–7.68 (13H, m), 8.15 (4H, br d, *J* 8, Ph) and 8.37 (4H, br d, *J* 8, Ph); δ_C (100 MHz; $CDCl_3$) 116.0 (C-Ar), 117.6 (C-Ar), 120.3 (C-*o*), 121.3 (C-*o*), 127.7 (C-*p*), 128.6 (C-Ar), 129.1 (C-*m*), 129.5 (C-*m*), 131.1 (C-*p*), 135.7 (C-*i*), 136.5 (C-*i*), 149.3 (Ar-C-N) and 154.3 (C^+); *m*/*z* 548 (M^+, 100%), 353 (34), 328 (34), 245 (8), 169 (48), 105 (PhN_2, 8) and 77 (Ph, 61).

***N*,*N*′-Bis(1,3-diphenyltetrazolium-5-yl)biphenyl-3,3′-diamide (8).** A mixture of 5-chloro-1,3-diphenyltetrazolium tetrafluoroborate (0.37 g, 1.1 mmol) and 3,3′-diaminobiphenyl[11] (0.20 g, 1.1 mmol) in acetonitrile (5.0 ml) was stirred at room temperature for 20 h. Aqueous NaOH (1 M, 30 ml) was added and the product was extracted with DCM and dried (Na_2SO_4). Then, the solvent was evaporated, giving a crude product (0.42 g), which was recrystallised from a chloroform–ethanol mixture to give the pure product (0.13 g, 38%) as a brick-red powder; mp 227 °C (dec.) (Found: C, 73.0; H, 4.5; N, 22.15. Calc. for $C_{38}H_{28}N_{10}$: C, 73.1; H, 4.5; N, 22.4%); ν_{max}/cm^{-1} 1622, 1564, 1490, 1468, 1368, 1330, 1288, 1206, 1160, 1112, 1070, 966, 758 and 680; λ_{max} (MeCN)/nm 262 (log ε 3.70), 302 (3.72) and 442 (2.74); δ_H (400 MHz; $CDCl_3$) 7.22 (2H, d, *J* 7.6), 7.32 (4H, m), 7.44 (12H, m), 7.78 (2H, t, *J* 1.8), 8.07 (4H, m) and 8.32 (4H, d, *J* 7.9); δ_C (100 MHz; $CDCl_3$) 119.9 (C-Ar), 120.0 (C-*o*), 121.1 (C-Ar), 121.2 (C-*o*), 122.1 (C-Ar), 127.8 (C-Ar or C-*p*), 128.6 (C-Ar or C-*p*), 129.1 (C-*m*), 129.5 (C-*m*), 131.1 (C-Ar or C-*p*), 135.4 (C-*i*), 136.3 (C-*i*), 142.4 (Cq-Ar), 149.1 (Ar-C-N) and 154.6 (C^+); *m*/*z* 624 (M^+, 0.3%), 404 (40) and 77 (Ph^+, 100).

Chemical reduction of 5 with zinc powder. A mixture of **5** (0.22 g, 0.39 mmol) and zinc powder (0.21 g, 3.2 mmol) was

ultrasonicated in DCM (6 ml) containing 15 drops of acetic acid for 20 min at room temperature. Aqueous NaOH (1 M) was added and the product was extracted with DCM. The extracts were dried (Na_2SO_4) and concentrated. The residue was purified by preparative TLC (alumina/DCM) to give **11** (79 mg, 46%) as deep-red crystals; mp 183–186 °C (Found: C, 70.0; H, 4.8; N, 25.4. Calc. for $C_{26}H_{22}N_8$: C, 69.9; H, 5.0; N, 25.1%); ν_{max}/cm^{-1} 3420, 1620, 1572, 1488, 1400, 1360, 1324, 1280, 1230, 1200, 1160, 1100, 1064, 960, 750 and 680; λ_{max} (MeCN)/nm 278 (log ε sh, 4.34), 309 (4.48) and 442 (3.38); δ_H (200 MHz; $CDCl_3$) 4.62 (3H, br s, NH and NH_2), 6.95–7.64 (15H, m, Ar and Ph), 8.16 (2H, m, Ph) and 8.34 (2H, br d, *J* 8, Ph); δ_C (50 MHz; $CDCl_3$) 120.3 (C-*o*), 121.7 (C-*o*), 124.0 (C-*o*), 124.1 (CH of Ar), 124.2 (C-*p*), 125.7 (CH of Ar), 128.4 (C-*p*), 129.4 (C-*m*), 129.8 (C-*m*), 130.0 (C-*m*), 131.2 (C-*i*), 131.6 (C-*p*), 135.3 (C-*i*), 136.4 (C-*i*), 143.2 (C-N), 147.3 (C-N), 152.3 (N-C-N) and 154.9 (C^+); *m*/*z* 446 (M^+, 0.02%), 328 (100) and 77 (89).

Chemical reduction of 9 with zinc powder. In a similar manner, **9** (0.10 g, 0.32 mmol) was reduced with zinc powder (0.10 g, 1.5 mmol) in DCM (5.0 ml) containing 15 drops of acetic acid. Aqueous workup and preparative TLC (alumina/DCM) gave *N*,*N*′-diphenylguanidine (53 mg, 78%) as colourless crystals; mp 144–150 °C (lit.,[12] 150 °C).

Acknowledgements

The Tübingen authors wish to thank VW-Stiftung, Hannover, for a grant (I/71009). We also have to thank Mr Paul Schuler for running EPR experiments and simulations. M. H. would like to thank Prof. Klaus Möbius for support, in particular for the use of the spectrometers, and Dipl. Phys. Jacob Lopez for his contribution to the ENDOR experiments.

References

1 For reviews on mesoionic compounds see: W. D. Ollis and C. A. Ramsden, *Adv. Heterocycl. Chem.*, 1976, **19**, 1; C. G. Newton and C. A. Ramsden, *Tetrahedron*, 1982, **38**, 2965; W. D. Ollis, S. P. Stanforth and C. A. Ramsden, *Tetrahedron*, 1985, **41**, 2239.
2 S. Araki, Y. Wanibe, F. Uno, A. Morikawa, K. Yamamoto, K. Chiba and Y. Butsugan, *Chem. Ber.*, 1993, **126**, 1149.
3 S. Araki, K. Yamamoto, M. Yagi, T. Inoue, H. Fukagawa, H. Hattori, H. Yamamura, M. Kawai and Y. Butsugan, *Eur. J. Org. Chem.*, 1998, 121.
4 For reviews on multi-stage redox systems see: K. Deuchert and S. Hünig, *Angew. Chem., Int. Ed. Engl.*, 1978, **17**, 875; S. Hünig and H. Berneth, *Top. Curr. Chem.*, 1980, **92**, 1; H. Perlstein, *Angew. Chem., Int. Ed. Engl.*, 1977, **16**, 519. For recent examples see: J. Zhou and A. Rieker, *J. Chem. Soc., Perkin Trans. 2*, 1997, 931; J. Zhou, M. Felderhoff, N. Smelkova, L. M. Gornostaev and A. Rieker, *J. Chem. Soc., Perkin Trans. 2*, 1998, 343.
5 For the singlet–triplet problem of similar systems see: A. Rebmann, P. Schuler, H. B. Stegmann and A. Rieker, *J. Chem. Res.* (*S*), 1996, 318; (*M*), 1996, 1765; A. Rebmann, J. Zhou, P. Schuler, A. Rieker and H. B. Stegmann, *J. Chem. Soc., Perkin Trans. 2*, 1997, 1615.
6 See, *e.g.* G. Frenking, A. Rieker, J. Salbeck and B. Speiser, *Z. Naturforsch.*, 1996, **51b**, 377.
7 See, *e.g.* A. R. Forrester and F. A. Neugebauer, in *Landolt–Börnstein, Numerical Data and Functional Relationships in Science and Technology*, ed. H. Fischer and K.-H. Hellwege, Springer-Verlag, Berlin, Heidelberg, New York, 1979, New Series, Group II: Atomic and Molecular Physics, Vol. 9, Magnetic Properties of Free Radicals, Part c1, Organic N-Centered Radicals and Nitroxide Radicals, pp. 51, 69, 75.
8 K. Möbius and R. Biehl, in *Multiple Electron Spin Resonance Spectroscopy*, ed. M. M. Dario and J. H. Freed, Plenum Press, New York, 1979, p. 475; K. Möbius, M. Plato and W. Lubitz, *Phys. Rep.*, 1982, **87**, 171.
9 M. Plato, W. Lubitz and K. Möbius, *J. Phys. Chem.*, 1981, **85**, 1202.
10 R. N. Hanley, W. D. Ollis and C. A. Ramsden, *J. Chem. Soc., Perkin Trans. 1*, 1979, 736.
11 C. C. Barker and F. D. Casson, *J. Chem. Soc.*, 1953, 4184.
12 J. Macholdt-Erdniss, *Chem. Ber.*, 1958, **91**, 1992.

Paper 8/09386E